Supplementary Materials for

Ecological suicide in microbes

Christoph Ratzke*[1†], Jonas Denk*[2] and Jeff Gore[1†]

[1] **Physics of Living Systems, Department of Physics, Massachusetts Institute of Technology, Cambridge, MA, USA**

[2] **Arnold-Sommerfeld-Center for Theoretical Physics and Center for NanoScience, Ludwig-Maximilians-Universität München, Theresienstraße 37, D-80333 München, Germany**

*equal contribution

[†] correspondence should be sent to: cratzke@mit.edu or gore@mit.edu

Supplementary Text

In these Supplementary Notes we further elaborate our dynamical analysis of ecological suicide in microbes. We first discuss the dependence of the fluorescence intensity of our fabricated nanobeads (see Methods) on the pH. Then, we present time resolved measurements of the optical density and the fluorescence intensity of these nanobeads throughout our daily dilution experiments.

To test our conceptual understanding of ecological suicide in *Paenibacillus sp.* (Ps), we present a mathematical description based on our experimental observations. We show that the proposed mathematical equations capture the complete phenomenology of ecological suicide in Ps, including non-monotonic growth dynamics and oscillatory behavior in daily dilutions.

Paenibacillus sp. isolation and phylogeny:

The *Paenibacillus sp.* was isolated from a grain of soil collected in Cambridge, MA, USA and was part of a soil species collection that will be described in more detail elsewhere (Logan Higgins et al, in prep). The 16S rRNA of this strain was sequenced and is most closely related to *Paenibacillus tundrae A10b* [1] according to RDB/SeqMatch tool [2] with a similarity score of 0.995 and a S_ab score of 0.975. For a characterization of all 21 species shown in Fig.4, please refer to Fig. S9. Also here we used the to RDB/SeqMatch tool and assigned the used bacteria to their closest related bacteria based in the maximal similarity score and S_ab.. For a characterization of all 21 species shown in Fig.4, please refer to Supplementary Fig. 9. Also here we used the to RDB/SeqMatch tool and assigned the used bacteria to their closest related bacteria based in the maximal similarity score and S_ab.

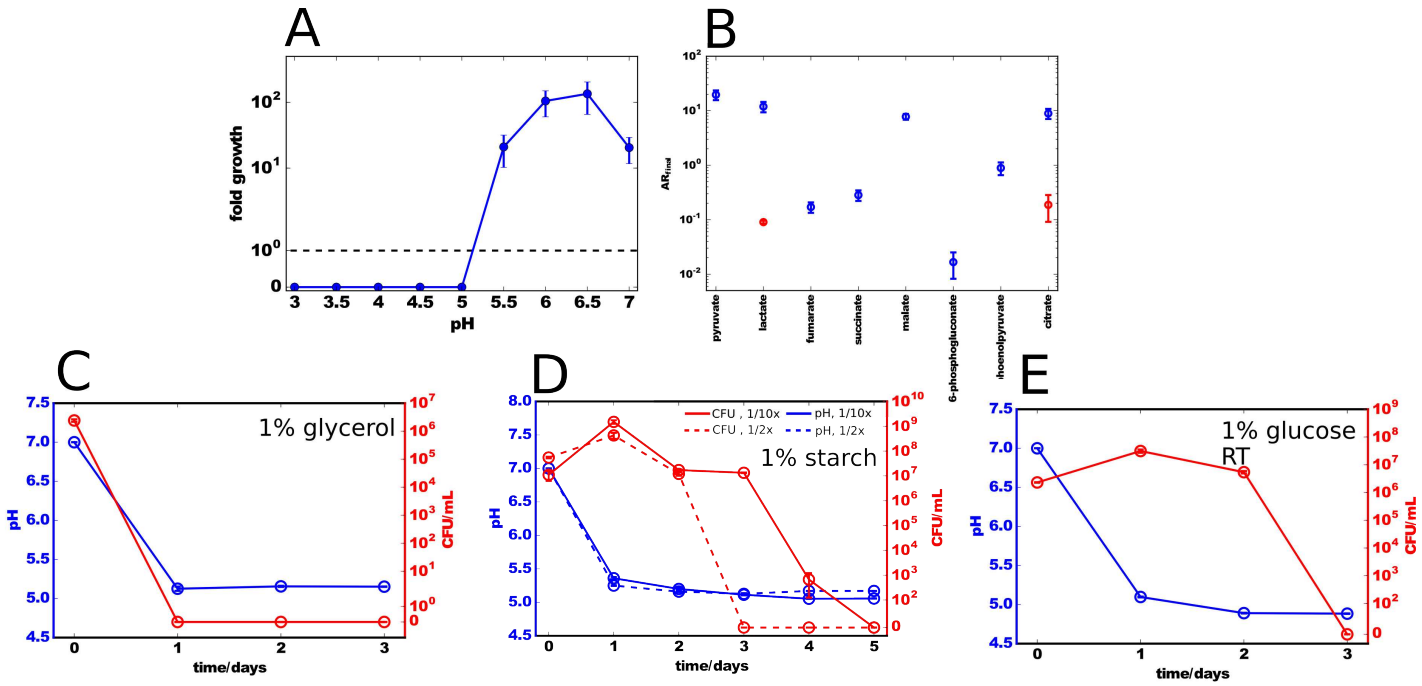

Supplementary Fig. 1: Growth of Paenibacillus sp. at different pH values, secretion of organic acids and ecological suicide under different conditions. *(A) The CFU were measured at the beginning and end of 24 hours of growth. The fold growth is the ratio of final/initial CFU. At low pH values the bacteria die. The horizontal dashed line marks a fold growth of 1 - eg the cell number did not change over 24 hours. The errorbars are SEM from three replicates. (B) Paenibacillus sp. was grown in M9 media with 2% glucose as the only carbon source. Mass spectrometry of the supernatant indicated that a variety of organic acids were produced by the bacteria. Pyruvate and lactate could be detected in the original media (red circles) but increased in concentration upon bacterial growth. Several other organic acids could not be detected in the original media but accumulated upon bacterial growth. Organic acid secretion can possibly be a result of a type of overflow metabolism*[9]*. AR is the area ratio of the area under the curve for the detected substance divided by the area under the curve of an internal standard (isotope labeled amino acid). Ecological suicide is observed on 1% glycerol (C), on the complex carbohydrate starch (D), and at room temperature, ~22°C (E). For (C) and (E) the experiment was performed similar to the experiments probing the ecological suicide on glucose and as described in the Methods, but with glycerol or at room temperature instead. For (D) Paenibacillus was grown in 0.5x Nutrient with 1% starch overnight and directly diluted 1/2x or 1/10x into the same medium with additional 1g/L* NH_4Cl*. The bacteria were grown at 30°C. The plots show mean and SEM of three replicates each.*

Paenibacillus sp. growth at different pH values and its production of organic acids

Paenibacillus sp. was pre-cultured in tryptic soy broth. The next day it was diluted into 1xNu with 100mM Phosphate pH7 and grown to OD2. After washing three times in Base medium with 10mM Phosphate the bacteria were adjusted to an OD of 2 and diluted 1/100x into Base medium with 100mM Phosphate with the pH ranging from 3 to 7. The CFU was measured at the beginning and after 24hours to obtaine a fold growth of the bacteria. As can be seen in Fig. S1A *Paenibacillus sp. c*annot grow at low pH values. This is in line with Fig. 1 where upon reaching a pH of around 5 the bacteria start to die and again shows that it is the pH that drive the ecological suicide.

To better understand how *Paenibacillus sp.* changes the pH of the medium we grew it in M9 buffer with 2 % Glucose as only carbon source. After 24hours the spent medium was analyzed with mass spectrometry. As can be seen in Fig. S1B a variety of organic acids could either be found to increase in concentration or to become detectable at all.

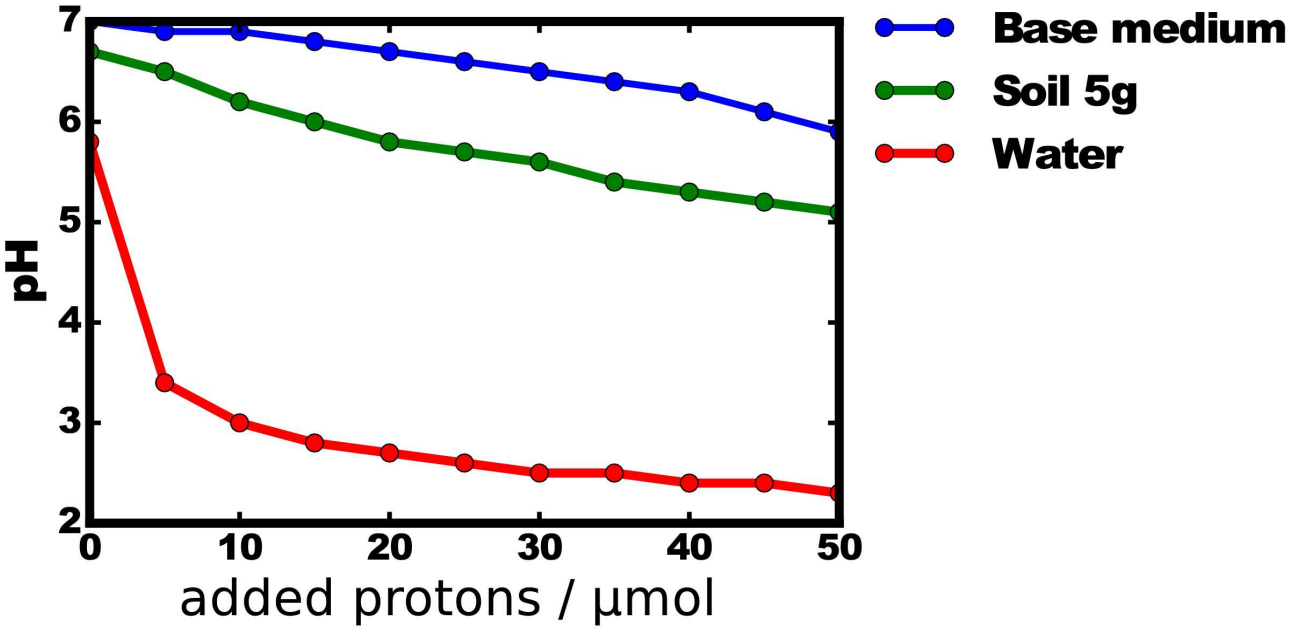

Supplementary Fig. 2: Buffer capacity of Base medium with 10mM Phosphate is higher than that of the soil the microbes were isolated from. *5g (wet weight) soil from the same location the microbes of this study were isolated from was dispersed in 15mL water. The pH of this dispersion was measured while hydrochloric acid was added. The obtained titration curve was compared with that of 5mL Base medium and pure water. As can be seen our medium is slightly stronger buffered than the soil.*

The proton concentration in a buffer system is given by:

$$H = \frac{K_d HA}{A}$$

with H as proton concentration, K_d as the dissociation constant and A as the base concentration. This can be converted by canceling out the volume into

$$H = \frac{K_d n_{HA}}{n_A}$$

Upon adding a small amount hydrochloric acid n_{HCl} this acid reacts with the acid and base present such that:

$$H_{new} = \frac{K_d (n_{HA} + n_{HCl})}{n_A - n_{HCl}}$$

from which the buffer capacity will be obtained as

$$\frac{-\log(H_{new}) + \log(H_{old})}{\Delta n_{HCl}}$$

Thus the buffer capacity is independent from the volume (and thus the soil can be diluted with water without affecting the buffer capacity) but just depends on the total amount of buffer, therefore the initial volume/mass for all samples was 5mL/5g.

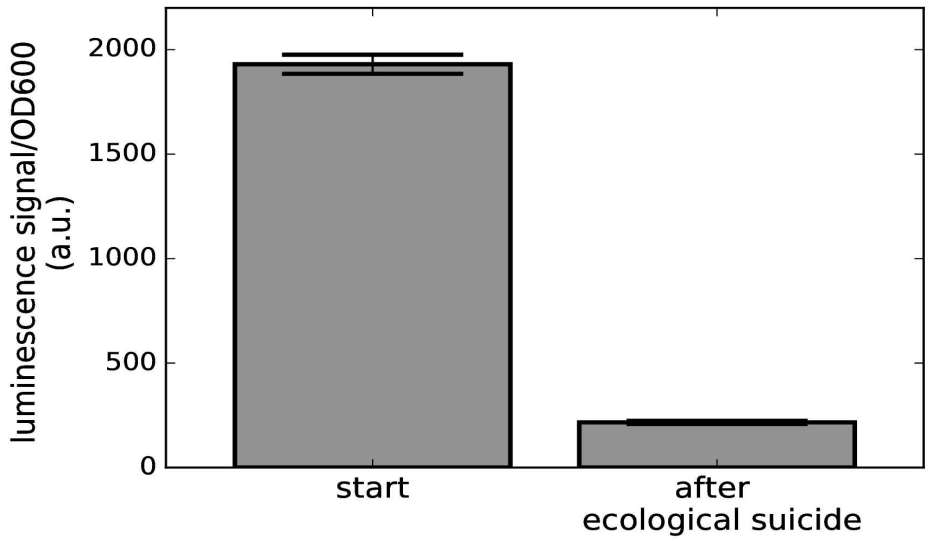

Supplementary Fig. 3: Cell viability assay confirms loss of viability upon ecological suicide. The BacTiter-Glo (Promega, Madison, USA) assay was used that measured the cellular ATP content as a indicator for cell viability. As all cell viability assays also this one has the disadvantage that cellular ATP levels to not have to be directly linked to cell viability. However, upon ecological suicide a drop of cellular ATP levels of around 90% could be observed. The final values were taken after 24hours in Base medium with 10mM Phosphate and 10g/L glucose. Bars show mean of 4 replicates and error bars show SEM.

Dependence of the nanobeads' fluorescence intensity on the pH:

To study the dynamics of the pH, we fabricated fluorescent nanobeads (see methods) which show a pH-dependent fluorescence intensity [3]. These nanobeads contain fluorescein, whose fluorescence intensity depends on the pH, and a highly photostable fluorinated porphyrin (TFPP), which acts as a red-emitting

pH independent reference dye. Since the fluorescence intensity of TFPP is independent of pH it serves as internal standard to make the result independent of the overall nanobead concentration. Thus, the ratio of the fluorescein and TFPP fluorescence signals is a function only of the pH value. Since in our 24-hours experiments the pH varied between 4 and 7, we measured the fluorescence intensity ratio of the nanobeads for different pH values in this range. The fluorescence intensity ratio increases monotonic for increasing pH. Moreover, the slope of the intensity ratio decreases for decreasing pH and the intensity seems to saturate for low pH (Fig. S4).

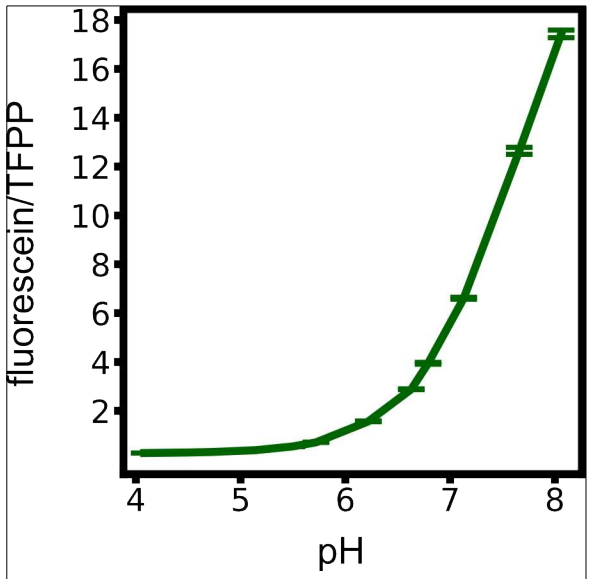

Supplementary Fig. 4: The nanobeads' fluorescence ratio of fluorescein and TFPP depends on the pH. *Rescaling the fluorescein signal with the TFPP signal shows a monotonic increase as a function of the pH. The fluorescence of the nanobeads was measured in base medium with adjusted pH values as shown on the x-axis. Errorbars show the SEM of 8 independent replicates.*

Dynamic measurements of the optical density and pH:

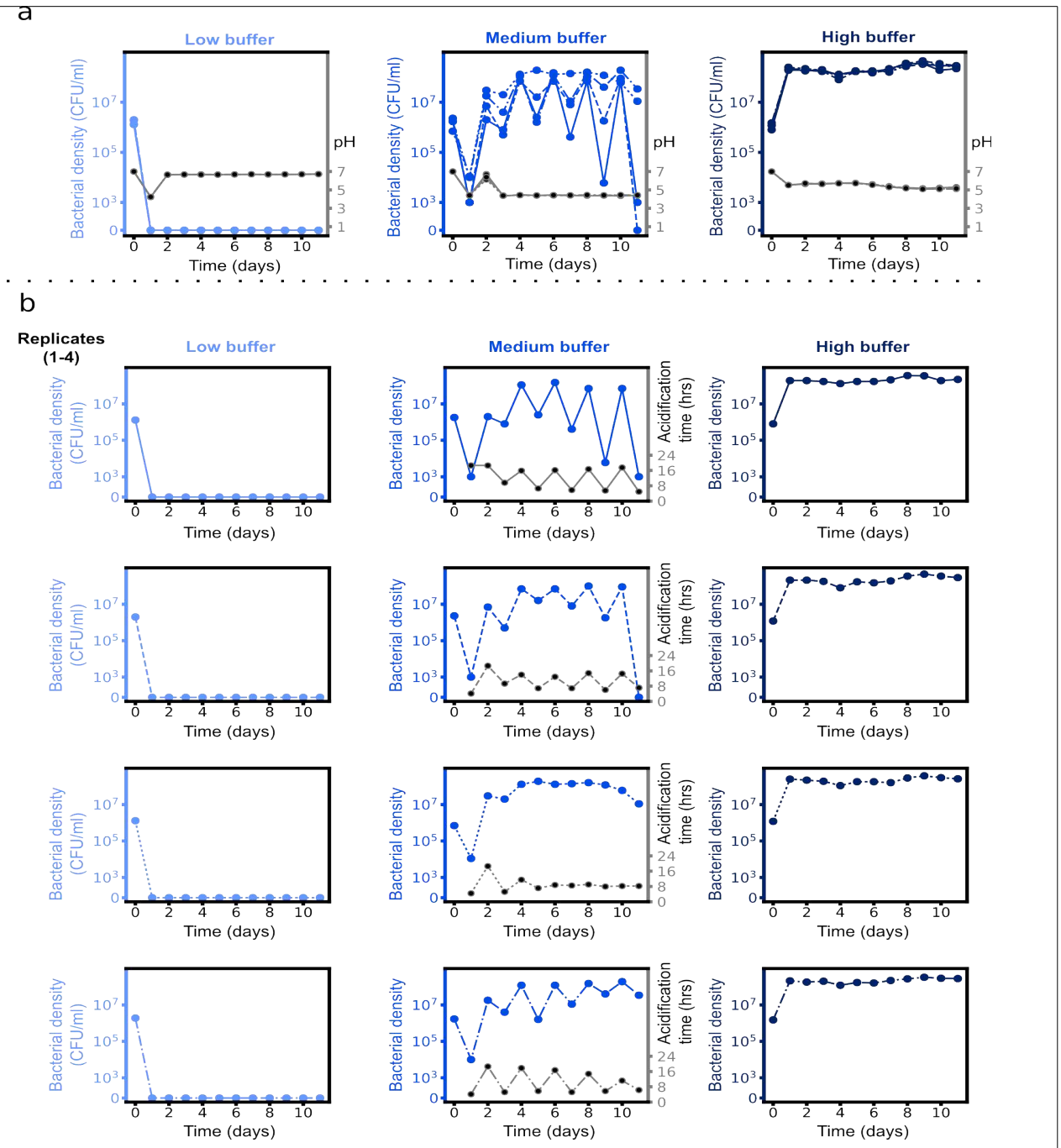

Supplementary Fig. 5: Population oscillations. *(a) Independent of the initial bacterial density, the daily final pH saturates at the same values. The four blue lines in (c-e) (solid, dashed, dotted, dashed-dotted) show the respective replica also shown in Fig. 2c-e. Instead of the acidification time we plot here the respective daily final pH values in grey (replicates are hardly distinguishable and the daily final pH of the replica are nearly identical). (b) Replicates of Fig. 2 c,d,e as separate plots.*

As detailed in the main text (Fig. 2c-e), our daily dilution experiments show oscillatory behavior of the bacterial density, which was measured at the end of each day. In contrast, we could not observe significant oscillations in the pH at the end of each day, i.e. for a certain buffer concentration, the pH after one day was approximately constant (Fig. S5).

This suggests that from the pH values at the end of each day it is not possible to infer the (oscillating) behavior of the bacterial density. Therefore, we also studied the dynamics of the pH during the course of each day during our daily dilution experiment. To this end, we prepared parallel experiments with the same buffer conditions and initial bacterial dilutions as for the daily dilution experiments (see Methods). In contrast to the daily dilution experiments, to these parallel experiments we also added fluorescent nanobeads and measured the optical density and fluorescence intensity of the nanobeads (see Methods). Whereas for the bacterial density (CFU/ml) at the end of each day we counted the living bacteria, the optical density provides a measurement for the total amount of bacteria (dead and alive). As detailed above (Fig. S4), the fluorescence intensity ratio of the nanobeads provides a measure for the pH.

For very low buffer concentrations (10mM phosphate), our daily dilution experiments (Fig. 2 left) display ecological suicide during the first day already. Consistently, in the corresponding parallel experiment with fluorescent nanobeads we find an early and strong decrease of the fluorescence intensity ratio after four hours of the first day already, indicating a strong decrease in pH (Fig. S6). This drop in pH is accompanied by a rapid increase of the optical density. On the second day (and all following days), the optical density mostly stays constant for the entire day. This strongly suggests that the bacteria have died on the first day already, which is underlined by finding no viable cells via plating on rich medium agar (Fig. 2c). In all measurements of the nanobeads' intensity ratio, we find an initial rapid increase. We argue that this initial increase is due to the initial increase in temperature during the

initial heating of the PlateReader to 30°C. When suspended in pure base (without bacteria) we indeed observed an increase of the fluorescence signal of the nanobeads for increasing temperature (Fig. S7).

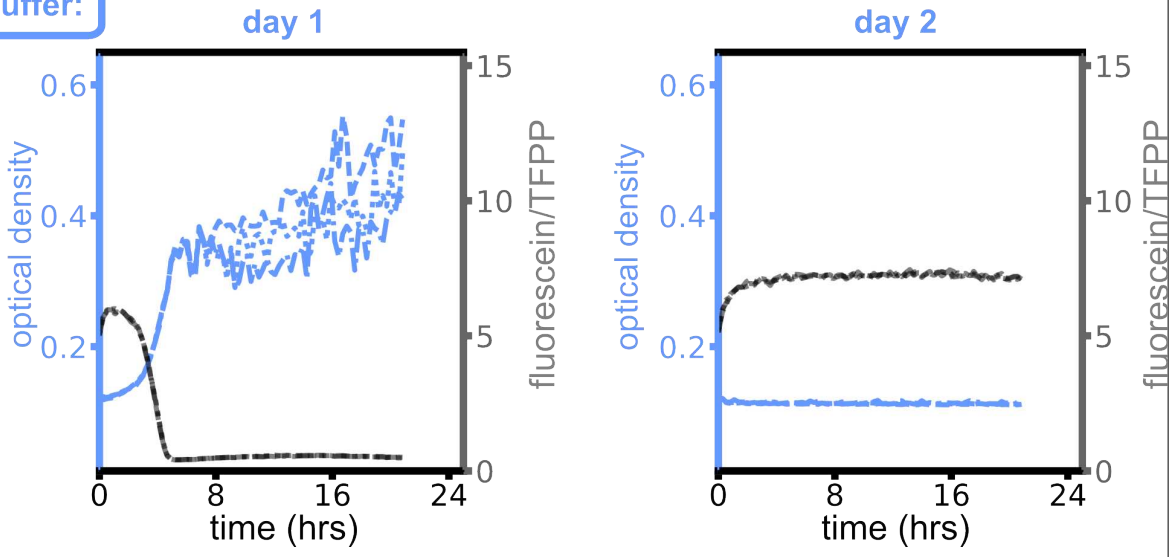

Supplementary Fig. 6: For low buffer concentrations (10mM phosphate), an early pH drop leads to ecological suicide. *The three sample curves (dashed, dotted, dotted-dashed) correspond to the samples of the daily dilution experiment in Fig. 2 of the main text for the first two days. The fluorescence intensity of fluorescein/TFPP drops after four hours already, eventually leading to ecological suicide on the first day. There was no background correction for the OD values which explains the nonzero OD on day 2.*

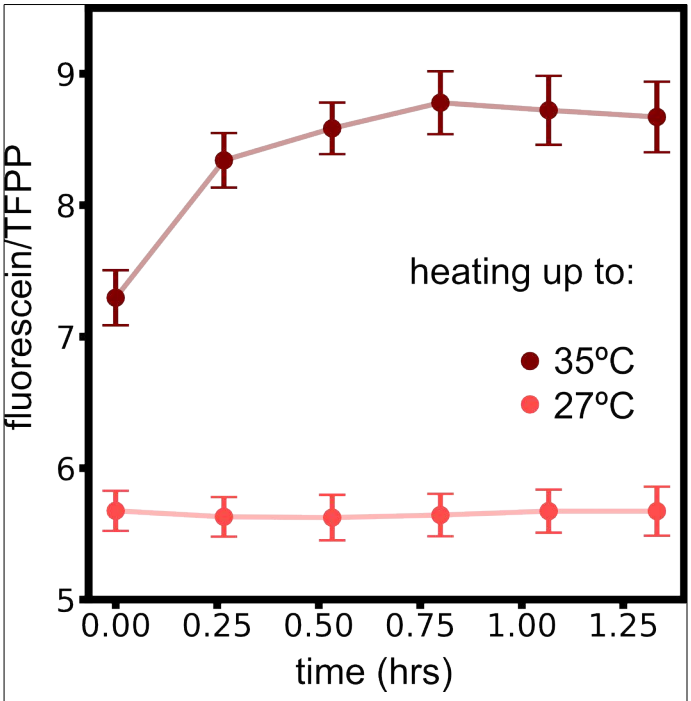

Supplementary Fig. 7: The fluorescence intensity ratio of the nanobeads is temperature dependent. *The temperature dependence rationalizes the initial increase of the fluorescence intensity ratio in Supplementary Fig. 6 and 8. The fluorescence of the nanobeads was measured over time in base buffer at pH 7. First the nanobeads were incubated at 27°C until a stable value could be obtained. Afterwards the temperature was increased to 35°C and the measurement continued. The increase in temperature is followed by a increase in the fluorescence ratio, which shows that the signal is temperature dependent. Mean and SEM of 10 replicates are shown.*

For high buffer concentrations, the optical density and the nanobeads' fluorescence intensity show a similar respective increase or decrease on each day (Fig. S8 a,c). This is consistent with the daily saturation of the bacterial density observed in our daily dilution experiments (Fig. 2e). As mentioned

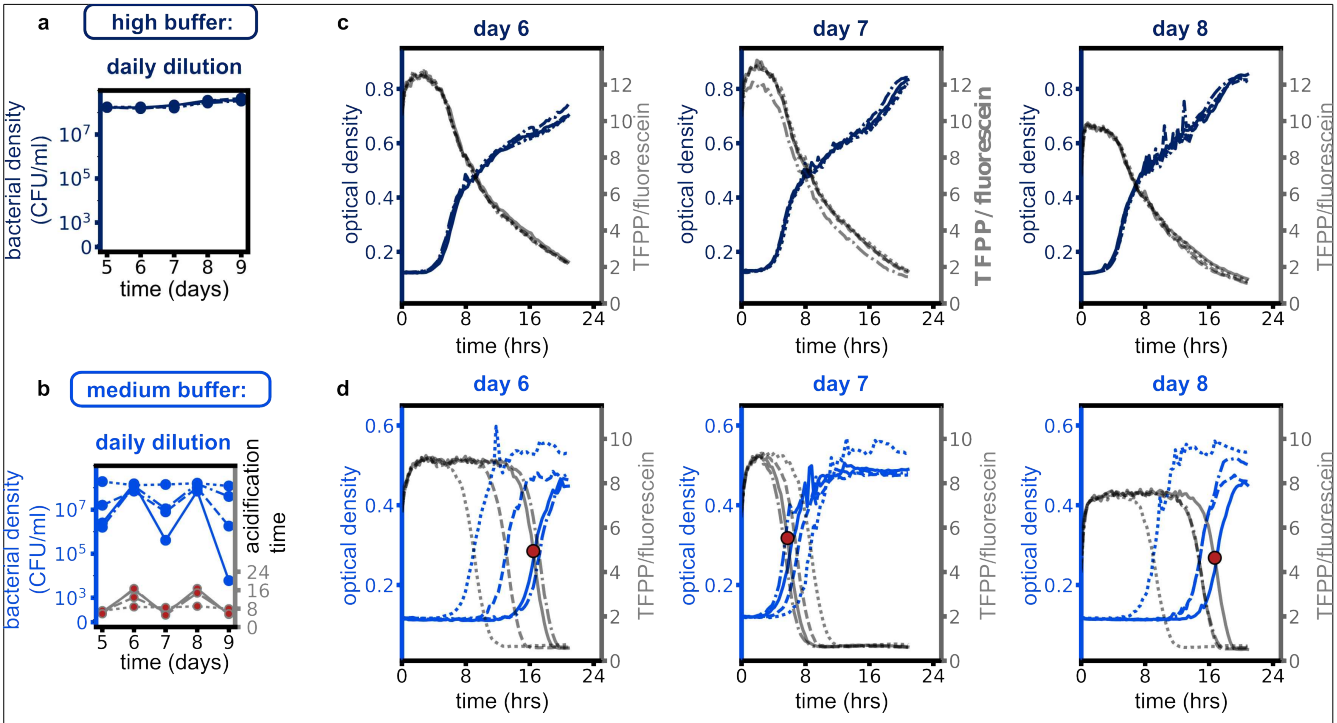

Supplementary Fig. 8: The acidification time oscillates with the bacterial density. (a-b) *The daily dilution experiments for high (100mM phosphate) and medium (26mM phosphate) buffer concentrations show daily saturation and oscillatory behavior of the bacterial density, respectively.* ***(c)*** *For high buffer concentrations, the fluorescence intensity and the optical density in the parallel experiments with fluorescent nanobeads show similar dynamics each day.* ***(d)*** *In contrast, for medium buffer concentrations the corresponding parallel experiments with fluorescent nanobeads reveal oscillations in the acidification time (red circle, shown for one sample represented by the solid line). The four different replica (solid, dotted, dashed, dotted-dashed) of these parallel experiments correspond to the respective replica shown in Fig. 2c-e.*

above, for intermediate buffer concentrations we could observe oscillations in the bacterial density but not in the pH at the end of each day (Fig. S5). However, our parallel experiments with fluorescent

nanobeads reveal oscillatory behavior of the time the fluorescence intensity--and thus also the pH--drops (acidification time, which is defined as the turning point of the resulting S-shaped fluorescence ratio curve). A late drop of the fluorescence is accompanied with a high final bacterial density in the daily dilution experiment and an early drop with a low final bacterial density. Hence, for intermediate buffer concentration the acidification time in our parallel experiment oscillates with the bacterial density in the daily dilution experiment (Fig. S8).

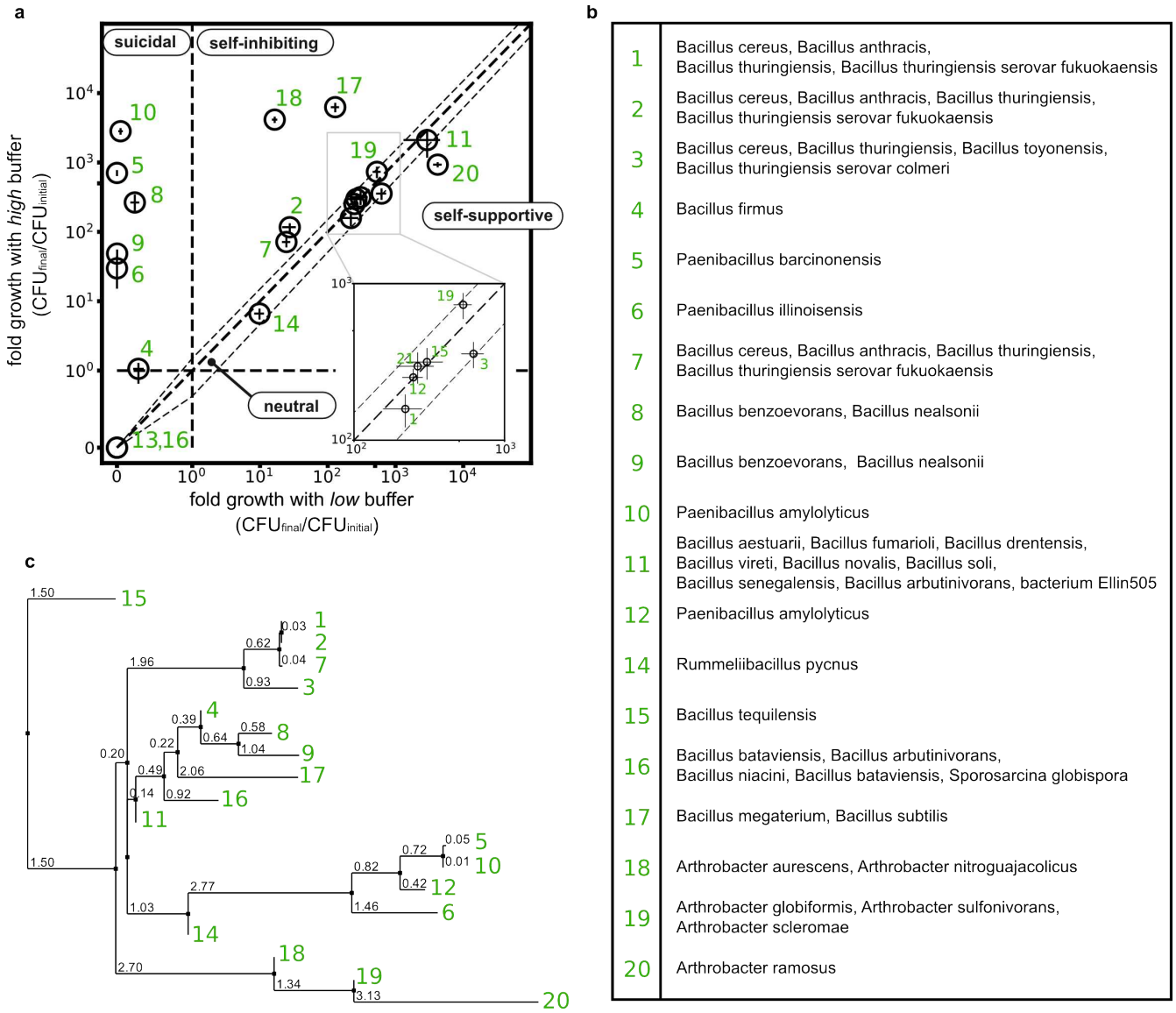

Supplementary Fig. 9: Relatedness of the used soil bacteria used to study the frequency of ecological suicide (Fig. 4 in main text) *(a) Categorization of the studied soil species as in Fig.4. The green numbers assign the individual species to their position in the phylogenetic tree (c). (b) Identification of the used species based on their 16s rRNA sequence according to RDB/SeqMatch tool [2]. The right column lists all respective related bacteria with maximal similarity score and S_ab score. (Sequencing of species 13 and 21 failed.) (c) Phylogenetic tree which shows the relatedness of the used bacteria. Green numbers stand for the species used in (a) and assigned in (b), black numbers show genetic distance. The* similarity matrix was calculated from the percentage identity (PID) between the sequences after multiple sequence alignment. The tree was build by neighbor joining method [8].

Mathematical approach to ecological suicide**:**

As detailed in the main text, our conceptual understanding of ecological suicide is based on the following principles: bacterial growth leads to a change in their environment (pH) in a way that eventually harms themselves and leads to their own death. Hence, bacteria experience a negative feedback mediated by the surrounding pH. It is important to note that we do not seek a complete description of ecological suicide including all the molecular details, but rather want to test our conceptual understanding (negative feedback) on a phenomenological level. Here, we show that from a mathematical perspective, ecological suicide is a very generic phenomenon, which can be captured by a minimal extension of previous mathematical descriptions of bacterial growth [5]. Bacteria have an optimal pH value where they grow best [8,9]. Deviations from this value deteriorate their growth and can even cause their extinction. To account for this pH dependence of bacterial growth, we propose the following dynamics for the bacterial density n:

$$\frac{dn}{dt} = \alpha n \left(1 - \frac{n}{\kappa}\right) \Gamma[p] \quad , \tag{1}$$

where α and κ are the growth rate and the carrying capacity, respectively, and the function $\Gamma[p]$ depends on the proton concentration p and represents the effect of the proton concentration (pH) on the bacterial growth. For a fixed $\Gamma[p]$, this equation is the well-studied logistic growth with growth rate $\alpha\Gamma[p]$ and carrying capacity κ . One ad hoc choice to account for a pH dependence of the bacterial growth is to assume that the deterioration of bacterial growth with changing proton concentration follows a Gaussian. Here, we define

$$\Gamma[p] := 1 - \left(\frac{1 - \exp\left[\frac{\left(p - p_{opt}\right)^2}{2\sigma^2} \right]}{1 - \exp\left[\frac{\left(p^c\right)^2}{2\sigma^2} \right]} \right) \quad , \tag{2}$$

where p_{opt} denotes the optimal proton concentration and p^c denotes some critical proton concentration deviation beyond which bacteria start to die. All of these proton concentrations are not in physical units but instead is simply meant to capture the dynamics of the proton concentration. σ determines how far from the optimal proton concentration the species can grow / survive. Based on the strong correlation between the increase in the optical density and the fluorescence intensity ratio (Fig. S6 and S8), we assume that the change in pH—and thus the proton concentration—is directly related to the growth of the bacteria. A naive assumption would therefore be that the change in proton concentration is simply proportional to the change in bacterial density and is completely determined by eq. (1). However, note that in this case the system reduces to a system of only one dynamic variable (the bacterial density n) which would not be able to reproduce non-monotonic growth [39] as observed in our experiments (Fig. 1). There are many ways to implement a negative feedback of the proton concentration on the bacterial density capable of reproducing non-monotonic behavior as observed in our experiments [4,5]. The goal of our mathematical description is not to account for the molecular details of the process, which would involve the complex (and largely unexplored) metabolism of the particular bacteria under consideration (in our case *Paenibacillus sp*.). In contrast, our goal is to develop a simple mathematical model that delivers intuition about the dynamics of ecological suicide in *Paenibacillus sp.* and test its consequences especially in the light of the experimental findings like non-montonous growth and oscillations.

Fig. 1c displays a decrease of the pH even after saturation of the bacterial density and thereby suggests, that the proton concentration also couples to the bacterial density itself. Since, in principle, the proton concentration could depend on both the change of the bacterial density $\left(\frac{dn}{dt}\right)$ and the bacterial density (n) itself, we make the following approach for the dynamics of p :

$$\frac{dn}{dt} = \beta_1 \left(\frac{dn}{dt} \right) \Theta \left[\frac{dn}{dt} \right] + \beta_2 n, \tag{3}$$

where β_1 and β_2 are (real, positive) coupling parameters. $\Theta[\cdot]$ denotes the Heaviside step function, which is one for a positive argument and zero otherwise and accounts for our assumption that bacteria increase the proton concentration during their growth, but do not affect the pH when they die. Whereas high β_1 and β_2 will yield a fast increase in the proton concentration with bacterial growth and total density respectively, for very low β_1 and β_2 the proton concentration will hardly change. We therefore assume a decrease of β_1 and β_2 to emulate an increase in buffer concentration in our experiments. This model is thus an extension of the simpler model used in [10]. Measuring time, bacterial density and proton concentration in units of $1/\alpha$, κ, and p_{opt}, respectively, the only independent parameters are the rescaled coefficients coupling p to $\frac{dn}{dt}$ and n given by $\beta_1' = \beta_1 \kappa / p_{opt}$ and $\beta_2' = \beta_2 \kappa / (\alpha\, p_{opt})$, respectively, the rescaled critical proton concentration deviation p^c / p_{opt}, and the rescaled spread σ / p_{opt}. Fig. S10 a-c show the dynamics of the bacterial density and the proton concentration as a function of time for a certain time interval $24/\alpha$,which is proposed to simulate daily growth. In all simulations we chose the same values for $p^c / p_{opt} = 0.6$ and $\sigma^2 / p^2_{opt} = 1$, assumed the initial proton concentration to be optimal and only varied the coupling coefficients β_1' and β_2'. For convenience, the proton concentration is plotted as $-\log(p)$, which is up to some scaling the corresponding pH of the system. Similar to our experimental observations for increasing the buffer concentration (compare to Fig.1 a-c), decreasing the coupling of the proton concentration to the bacterial density (by lowering β_1' and β_2') shows a transition from a rapid decline of the bacterial density for strong coupling to saturation of the bacterial density at the carrying capacity for weak coupling (Fig. S10 a-c). Note, that due to the continuous

description, the bacterial density n cannot reach 0 (extinction) but only approaches 0 at infinite times. However, from our daily dilution experiments (Fig. 1c) we can estimate the carrying capacity with approximately 10^8 cells; hence bacterial densities below $1/10^8\kappa$ would correspond to less than one cell. We therefore claim that bacterial densities below $1/10^8\kappa$ correspond to extinction in our experiments and manually set the bacterial density to zero, if it is lower than $1/10^8\kappa$. Starting at different initial conditions, the fold growth of the bacteria is decreasing for increasing initial concentrations (Fig. S10 d), as observed in our experiments (Fig. 2a). Similarly, there is a critical maximal initial density above which the bacteria start to die out (the fold growth drops below 1). Eqs. (1)-(3) were solved for different initial bacterial densities and proton concentrations as well as different rescaled coupling coefficients $\beta_1^{'}$ and $\beta_2^{'}$ using NDsolve[] in Wolfram Mathematica 11. Similar to our experiments, this reciprocal dependence of the initial to the final density leads to interesting behavior when simulated in a "daily dilution" simulation: Here, we numerically integrated equations (1) to (3) for $24/\alpha$, which in line with our above simulations represents one day of our experiments. To account for the 1/100x daily dilution, the final bacterial concentration is multiplied by a factor of 1/100 and then taken as the initial bacterial density of the subsequent simulation. Note, that this procedure can be understood as a discrete map for the bacterial density, where - apart from the dilution factor of 1/100 - the mapping is given by the relation of the bacterial density at t= $24/\alpha$ and $t=0$ as given in Fig. S6d. Discrete maps show a rich phenomenology ranging from stable fixed points and limit cycles to chaos and can be very sensitive to the form of the mapping function [6]. Similarly, we expect that changing the form of the mapping function (Fig. S10 d) by changing the coupling constants $\beta_1^{'}$ and $\beta_2^{'}$ is critical for the long-term behavior in our daily dilution simulations. In view of the similar shapes of this mapping (Fig. S10 d) and the well-studied logistic map [7]we speculate that for a very shallow shape--as it occurs for weak coupling (small $\beta_1^{'}$ and $\beta_2^{'}$)--the discrete map approaches a stable fixed point, whereas for a steep (negative) slope due to strong coupling (large

β_1' and β_2') the bacterial density will diverge until it eventually takes values below $1/10^8 \kappa$ (extinction). For intermediate slopes, i.e. for intermediate values for β_1' and β_2' , the daily dilution simulations may show oscillations between multiple values (Fig. S10 g). Fig. S11 shows respective bifurcation diagrams of our daily dilution simulations when varying the coupling constants β_1' and β_2' continuously. These bifurcation diagrams display bifurcations from one stable fixed point to oscillations between two values of the bacterial density. Also our experiments suggest bifurcations between a fixed final bacterial density and oscillations between multiple values (Fig. S12). Due to the sensitivity of logistic maps against a change in the mapping function and due to natural noise in our experiments, we note however that a quantitative categorization of the oscillations observed in our experiments (Fig. 2d) in terms of limit cycles of the underlying discrete map (Fig. 2a) may not be feasible and is beyond the scope of this work.

In our daily dilution simulations, for very strong coupling of the proton concentration to the bacterial density ($\beta_1'=3, \beta_2'=1$), the bacterial density dramatically decreases on the first "simulation day" already (Fig. S10 f). Due to our continuous description, the bacterial density does not reach zero. However, note that the bacterial density drops below $1/10^8 \kappa$, which corresponds to extinction as detailed above (to account for this extinction, we therefore manually set the density to zero). For medium coupling ($\beta_1'=0.3, \beta_2'=0.1$), we find oscillations in the final bacterial density (Fig. S10 g), reminiscent to our daily dilution experiments with intermediate buffer concentration (Fig. 2d). Furthermore, we find, that the acidification time (the time of the turning point in the proton concentration) oscillates with the bacterial density. For weak coupling ($\beta_1'=0.06, \beta_2'=0.02$), the bacterial density saturates at the carrying capacity after the first day already and all subsequent "simulation days" (Fig. S10 h), as observed in our experiments with high buffer concentration (Fig. 2e). The phenomenological agreement between our mathematical description and our experiments strongly

suggests, that the coupling of the bacterial density and the environment (here the pH) and the resulting non-monotonic growth dynamics are key aspects in understanding the phenomenon of ecological suicide.

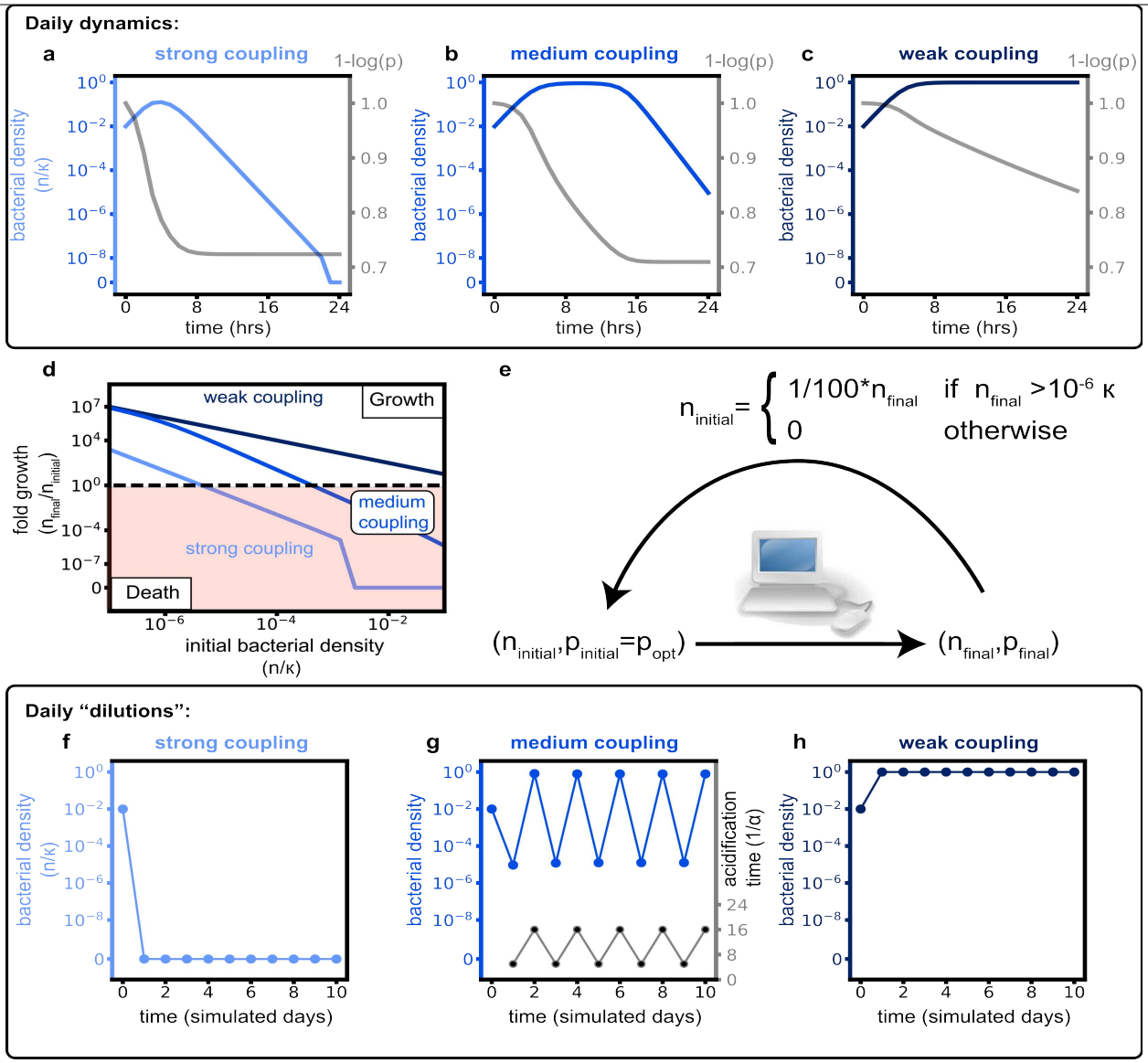

Supplementary Fig. 10: Negative feedback of the pH on the bacterial density suffices to recapitulate the phenomenology of ecological suicide as observed experimentally. a-c, Based on eq. (1)-(3), strong ($\beta_1^{'}=3, \beta_2^{'}=1$), medium ($\beta_1^{'}=0.24, \beta_2^{'}=0.08$), and weak ($\beta_1^{'}=0.06, \beta_2^{'}=0.02$ coupling has a similar effect on the growth dynamics as low, medium and high buffer concentrations in our experiments (Fig. 2c-e). **d,** The fold bacterial growth decreases for increasing initial concentration. When simulated in a "daily dilution" scheme. If the cell number that is 'diluted' at the end of the day dropped below one cell – this is possible since the variables are continuous in differential equitations -the bacterial density was set to zero. **e**, this reciprocal dependence leads to similar scenarios, **f-h,** as observed experimentally (Fig. 2, c-e).

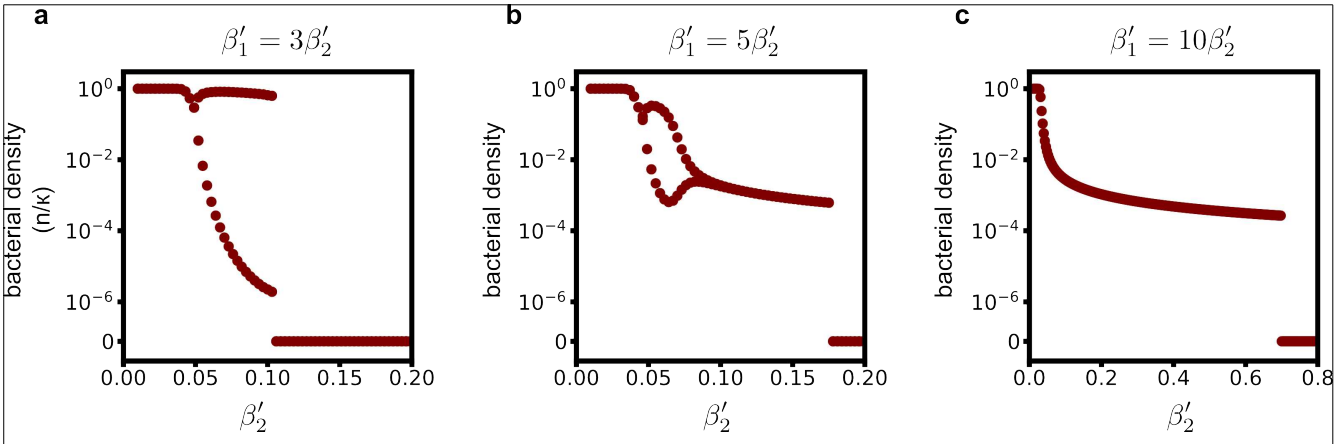

Supplementary Fig. 11: Varying the coupling constants β_1' and β_1' shows bifurcations from one fixed point to oscillations between two points. The bifurcation diagrams show the values of the bacterial density at the end of the last two days after 'daily dilution' simulations corresponding to 60 days. **a,** For comparable coupling constants (here: $\beta_1'=3\beta_2'$, as used in Fig. S6), the discrete mapping of 'daily dilution' simulations displays a bifurcation from one stable fixed point (saturation) to oscillations between two points. When a 1/100 dilution would cross the cutoff of $1/10^8\kappa$ (i.e. if after any of the 60 simulation days $n<1/10^6\kappa$), the bacterial density was manually set to zero. **b,** For an intermediate ratio $\beta_1'/\beta_2'=5$, the amplitude of oscillations first increases and then decreases again for increasing β_2' . **c**, For high enough β_1'/β_2' (here: $\beta_1'/\beta_2'=5$) the coupling to the change of bacterial density is dominant and the system saturates at low final densities, but shows no oscillations (recall that strong enough coupling to the bacterial density itself is crucial in our equations (3) to generate oscillations). In b, and c, the bacterial density drops below the extinction cutoff after the first first day already when β_2' is too high.

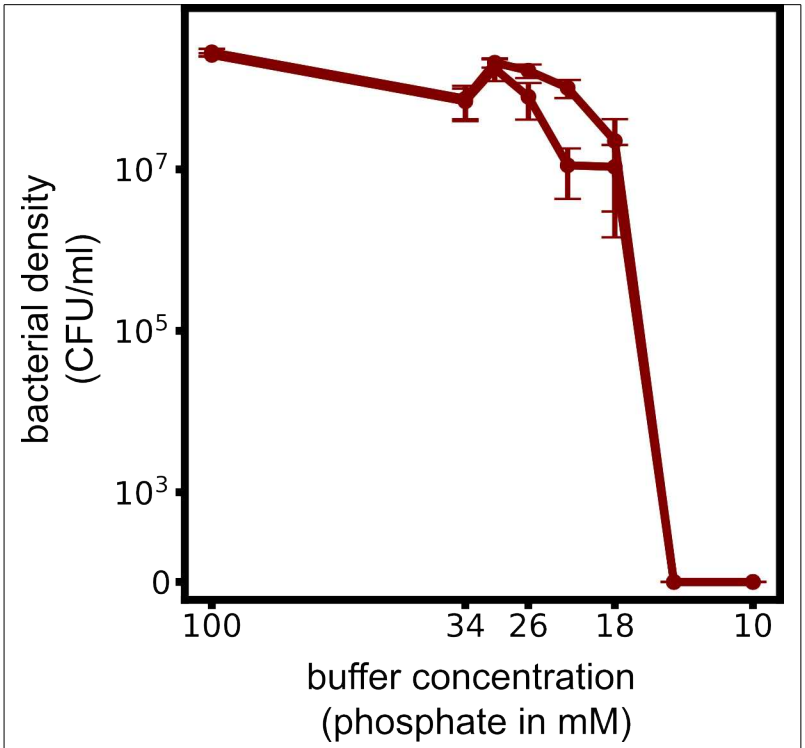

Supplementary Fig. 12: Experiments suggest a bifurcation between stable bacterial density at the end of each day and oscillations. The 'bifurcation diagram' shows the mean amplitude of the final bacterial density on the last day (day 11) and the second last day (day 10) for different buffer concentrations. The mean and SEM of the 4 replicates also used in Fig. 2 are shown.

References:

1. Nelson, D. M., Glawe, A. J., Labeda, D. P., Cann, I. K. O. & Mackie, R. I. Paenibacillus tundrae sp. nov. and Paenibacillus xylanexedens sp. nov., psychrotolerant, xylan-degrading bacteria from Alaskan tundra. *Int. J. Syst. Evol. Microbiol.* **59,** 1708–1714 (2009).

2. Cole, J. R. *et al.* Ribosomal Database Project: data and tools for high throughput rRNA analysis. *Nucleic Acids Res.* **42,** D633–D642 (2014).
3. Wang, X., Meier, R. J. & Wolfbeis, O. S. Fluorescent pH-Sensitive Nanoparticles in an Agarose Matrix for Imaging of Bacterial Growth and Metabolism. *Angew. Chem. Int. Ed.* **52,** 406–409 (2013).
4. Strogatz, S. H. *Nonlinear Dynamics and Chaos: With Applications to Physics, Biology, Chemistry, and Engineering*. (Westview Press, 2014).
5. May, R. M., Conway, G. R., Hassell, M. P. & Southwood, T. R. E. Time Delays, Density-Dependence and Single-Species Oscillations. *J. Anim. Ecol.* **43,** 747–770 (1974).
6. Hilborn, R. C. *Chaos and Nonlinear Dynamics: An Introduction for Scientists and Engineers*. (Oxford University Press, 2000).
7. May, R. M. & others. Simple mathematical models with very complicated dynamics. *Nature* **261,** 459–467 (1976).
8. Saitou, N. & Nei, M. The neighbor-joining method: a new method for reconstructing phylogenetic trees. *Mol. Biol. Evol.* **4,** 406–425 (1987).
9. Basan, M. *et al.* Overflow metabolism in *Escherichia coli* results from efficient proteome allocation. *Nature* **528,** 99 (2015).